Proteomics reveals a switch in CDK1-associated proteins upon M-phase exit during the Xenopus laevis oocyte to embryo transition.

Gaëlle Marteil, Jean-Philippe Gagné, Ewa Borsuk, Laurent Richard-Parpaillon, Guy G. Poirier, Jacek Kubiak

Submitted to "The International Journal of Biochemistry & Cell Biology", 11th May 2011, Revised 9th September, 2011, accepted 15th September, 2011.

Proteomics reveals a switch in CDK1-associated proteins upon M-phase exit during the *Xenopus laevis* oocyte to embryo transition

Gaëlle Marteil[1,2], Jean-Philippe Gagné[3], Ewa Borsuk[4], Laurent Richard-Parpaillon[1,2] , Guy G. Poirier[3] & Jacek Z. Kubiak[1,2]

[1] CNRS, UMR 6061, Institute of Genetics and Development of Rennes, Cell Cycle Group, F-35043 Rennes, France.

[2] University Rennes 1, UEB, IFR 140, Faculty of Medicine, F-35043 Rennes, France.

[3] Axe cancer, CHUQ Research Center, Faculty of Medicine, Laval University, 2705 Boulevard Laurier, Québec, Canada, G1V 4G2.

[4] Department of Embryology, Institute of Zoology, Faculty of Biology, University of Warsaw, Warsaw, Poland.

A B S T R A C T

Cyclin-Dependent Kinase 1 (CDK1) is a major M-phase kinase which requires the binding to a regulatory protein, Cyclin B, to be active. CDK1/Cyclin B complex is called M-phase Promoting Factor (MPF) for its key role in controlling both meiotic and mitotic M-phase of the cell cycle. CDK1 inactivation is necessary for oocyte activation and initiation of embryo development. This complex process requires both Cyclin B polyubiquitination and proteosomal degradation via the ubiquitin-conjugation pathway, followed by the dephosphorylation of the monomeric CDK1 on Thr161. Previous proteomic analyses revealed a number of CDK1-associated proteins in human HeLa cells. It is, however, unknown

whether specific partners are involved in CDK1 inactivation upon M-phase exit. To better understand CDK1 regulation during MII-arrest and oocyte activation, we immunoprecipitated (IPed) CDK1 together with its associated proteins from M-phase-arrested and M-phase-exiting *Xenopus laevis* oocytes. A mass spectrometry (MS) analysis revealed a number of new putative CDK1 partners. Most importantly, the composition of the CDK1-associated complex changed rapidly during M-phase exit. Additionally, an analysis of CDK1 complexes precipitated with beads covered with p9 protein, a fission yeast *suc1* homologue well known for its high affinity for CDKs, was performed to identify the most abundant proteins associated with CDK1. The screen was auto-validated by identification of: i) two forms of CDK1: Cdc2A and B, ii) a set of cyclins B with clearly diminishing number of peptides identified upon M-phase exit, iii) a number of known CDK1 substrates (e.g. peroxiredoxine) and partners (e.g. HSPA8, a member of the HSP70 family) both in IP and in p9 precipitated pellets. In IP samples we also identified chaperones, which can modulate CDK1 three-dimensional structure, as well as calcineurin, a protein necessary for successful oocyte activation. These results shed a new light on CDK1 regulation via a dynamic change in the composition of the protein complex upon M-phase exit and the oocyte to embryo transition.

1. Introduction

MPF (M-phase Promoting Factor) is the universal molecular regulator of M-phase progression (Masui and Markert, 1971). Identification of the molecular nature of MPF was possible due to the appropriateness *Xenopus laevis* oocytes appropriateness for biochemical analysis. MPF is composed of a kinase, CDK1 (Cyclin-Dependent Kinase 1), and a regulatory subunit, Cyclin B (Gautier *et al.*, 1988; Lohka *et al.*, 1988). CDK1/Cyclin B is associated with a third component of the complex, the p9 protein (Xe-p9 in *Xenopus*, Cks1 and Cks2 in mammals, orthologues of fission yeast Suc1 protein; van Zon et al. 2010.). The activation of CDK1 triggers M-phase entry, whereas its inactivation is linked to M-phase exit (Labbe et al., 1989; Riabowol et al., 1989). In *Xenopus*, CDK1 is activated during oocyte maturation and inactivated upon fertilization triggering embryo development. The sperm entry or a parthenogenetic treatment trigger an increase in intracellular free Ca^{2+} concentration promoting CDK1 inactivation that allows MII exit and the beginning of embryo development. This inactivation is due to the dissociation of CDK1/Cyclin B complex, Cyclin B degradation and CDK1 Thr-161 dephosphorylation (Nishiyama et al., 2000; Chesnel *et al.*, 2006; Chesnel *et al.*, 2007). More precisely, the APC/C (Anaphase-Promoting Complex/Cyclosome)-

dependent polyubiquitination of cyclin B targets the fully active CDK1/Cyclin B complex to the 26S proteasome. The 19S regulatory particle of the proteasome unfolds and dissociates Cyclin B from CDK1 (Nishiyama et al., 2000; Chesnel et al., 2006). Cyclin B dissociation is the earliest and indispensable step of CDK1 inactivation. Once separated from CDK1, Cyclin B is degraded, whereas the kinase is dephosphorylated on Thr-161 by type 2C protein phosphatase (Chesnel *et al.*, 2007). Both CDK1 Thr-161 dephosphorylation and Cyclin B degradation ensure the irreversibility of CDK1 inactivation. CDK1 inactivation requires its T-loop refolding, which closes the access of the kinase enzymatic active site. This closure may be mediated by chaperones, assuring the rapidity of CDK1 inactivation (reviewed in Kubiak and El Dika, 2011). Thus CDK1 inactivation may require modifications in association with different partners.

The increasing knowledge on CDK1 makes the hypothesis of a role of CDK1-specific inhibitors and/or chaperones in CDK1 inactivation very attractive. In mammals, two types of CDK inhibitors (CKIs) have been described (for review see De Clercq and Inze, 2006). The Ink4 family inhibits CDK4 and CDK6 by binding to CDK instead of Cyclin (McConnell *et al.*, 1999; Parry *et al.*, 1999), while Cip/Kip family members bind to and inhibit CDK/Cyclin complexes (Chen *et al.*, 1995). In *Saccharomyces cerevisiae*, Cdc6 in cooperation with Sic1 and Hct1 were postulated to participate in timely Cdc28 (CDK1-homologue) inhibition (Calzada *et al.*, 2001). This function has been recently suggested by Yim and Erikson (2011) in HeLa cells, but has never been shown in developmentally-regulated processes or in *Xenopus*. However, the CDK1 inhibitory role of Cdc6 remains controversial even in yeast (Archambault *et al.*, 2003). No other CKI has ever been shown to regulate mitotic CDK1 activity, and we wondered whether such regulators could exist during M-phase and participate in the regulation of CDK1 regulation in *Xenopus*.

Our goal in the present study was to identify CDK1 interactors during M-phase-arrest and upon oocyte activation leading to the entry into the first embryonic interphase. For several reasons, this transition in *Xenopus laevis* oocytes provides a unique opportunity for the biochemical study of putative changes in the composition of the CDK1 complex. First, the transition from active to inactive CDK1 is easily inducible and highly synchronous. Second, *Xenopus laevis* oocyte cytoplasm is abundant and rich in proteins (Nishiyama et al., 2000; Chesnel et al., 2006; Chesnel et al., 2007). The feasibility of proteomic analysis of such oocytes and embryos was already demonstrated by our previous MS study of ubiquitinated *X. laevis* proteins (Bazile et al. 2008). Our results show that the composition of the CDK1 complex is indeed modified during CDK1 inactivation and consequently these data open new

avenues for studying the function of so far unknown protein associations with this major M-phase regulator.

2. Materials and Methods

2.1. Egg collection and activation

Xenopus laevis females were purchased from NASCO (Fort Atkinson, WI). Females were subcutaneously injected with human chorionic gonadotropin (hCG, 500 IU/female). Unfertilized eggs (UFEs) were collected and washed with F1 buffer (31.25 mM NaCl, 1.75 mM KCl, 60 µM $MgCl_2$, 2 mM $NaHCO_3$, 10mM Hepes, 0.25 mM $CaCl_2$, pH 7.6). UFEs were dejellied with 2% L-cysteine in F1 buffer, pH 7.8. Aliquots of 200 UFEs for both CDK1 IP and p9 precipitation and of 20 UFEs for Western blotting analysis were made and frozen in liquid nitrogen. Eggs were activated using 0.5µg/mL calcium ionophore A23187 for 90 sec. Aliquots of 200 activated UFEs were taken out about 7 min after ionophore treatment for both CDK1 IP and p9 precipitation, and aliquots of 20 eggs were taken out 3, 7, 9, 15 and 30 min after treatment for Western blotting analysis.

2.2 Samples preparation for Western blotting

Eggs were homogenized in MPF-stabilizing buffer (80mM β-glycerophosphate, 50 mM NaF, 20 mM EGTA, 20 mM Hepes, 15mM $MgCl_2$, 1mM DTT, pH 7.5) with mixture of protease inhibitors (1mM AEBSF and 10µg/mL of aprotinin, leupeptin, pepstatin) and 10µg/mL of sodium orthovanadate and centrifuged (10000 g, 15 min, 4°C). The egg extract was mixed with Laemmli buffer (Laemmli, 1970), heated at 85°C and stored at -20°C.

2.3. CDK1 immunoprecipitation

To IP CDK1 during M-phase and M-phase exit, we used protein extracts of unfertilized (200 UFE) and activated eggs (200 eggs at 7 min post activation). Affi-Prep protein A beads were washed three times with TBS-Triton X100 (50mM Tris-HCl, 150 mM NaCl, 0.01% Triton X100, pH 7.5). The beads were then pre-equilibrated with or without (for IP negative control and for pre-clearing step) rabbit polyclonal antibody raised against *Xl*CDK1 C-terminal peptide (a gift from T. Lorca, CRBM, Montpellier, France), overnight at 4°C in TBS-Triton

X100 (50mM Tris-HCl, 150 mM NaCl, 0.01% Triton X100, pH 7.5), supplemented with proteases inhibitors and sodium orthovanadate (as above). We selected this antibody because it was previously successfully used to specifically immunoprecipitate CDK1 from *X. laevis* oocytes (Krasinska et al. 2008). Fifteen hours later, aliquots of 200 eggs were homogenized in 1mL of immunoprecipitation buffer (20mM Tris-HCl, pH 7.5, 150 mM NaCl, 10% glycerol, 2mM EDTA, 50 mM NaF, 50mM β-glycerophosphate, 0.2% NP-40) and centrifuged at 10 000g for 15 min at 4°C. Protein extracts were centrifuged again at 10 000g for 15 min at 4°C. Volumes of protein extracts were adjusted to 2 mL with IP buffer containing protease inhibitors, and a 15µl aliquot was collected for Western blotting analysis ("total fraction"). After three brief washes with IP buffer, naked beads (200µL per protein extract) were incubated with protein extracts and the mixture was agitated for 2 hours at 4°C to pre-clear the extract. The mixture of naked beads and egg extracts was then centrifuged at 4000 rpm, 3 min, 4°C. The supernatants were mixed with 100µL of naked beads (IP negative control) or of Affi-Prep protein A beads cross linked to CDK1 antibodies (dimethyl pimelimidate dihydrochloride was used as cross linking agent) previously washed twice with homogenizing buffer and agitated for 2.5 hours at 4°C. After centrifugation (1300g, 3 min, 4°C), the supernatants were kept for a second round of IP, but an aliquot of 15µL for each supernatant was conserved for Western blotting analysis ("unbound fraction"). The pellets were washed three times with 1.5 mL of TBS-Triton X100 with protease inhibitors. Proteins were eluted from beads using 100µL of 100mM glycine, pH 2.0. The eluted proteins were frozen at -20°C and the beads were eluted a second time with glycine and washed three times with TBS-Triton X100 and two times with IP buffer. The additional round of IP was performed as previously described by incubating the supernatant of the first round with the beads. The two aliquots of eluted proteins were pooled and neutralized with 1M Tris-HCl, pH 9.2. Laemmli buffer was added and the samples were heated at 85°C for 5min. A small aliquot was retained for Western blot analysis (bound fraction) and the remaining was analyzed by mass spectrometry.

2.4. CDK1 precipitation with p9 beads

To precipitate CDK1 with p9 beads during M-phase and M-phase exit, we used protein extracts made from unfertilized (200 UFE) and activated eggs (200 eggs taken out 7 min. after activation). p9-Sepharose beads were a kind gift from L. Meijer and O. Lozach (Marine Station, Roscoff, France; Vogel et al. 2002). p9-bound beads and naked Sepharose beads for

pre-clearing were pre-equilibrated overnight at 4°C in homogenizing buffer (25mM MOPS, pH 7.2, 60mM β-glycerophosphate, 15mM EGTA, 15mM $MgCl_2$, 2mM DTT, 1mM NaF, 1mM sodium orthovanadate) with protease inhibitors and 1% BSA. Aliquots of 200 eggs were homogenized in 0.8 mL of homogenizing buffer and centrifuged at 10 000g for 15 min at 4°C. Protein extracts were centrifuged at 10 000g for 15 min at 4°C. Volumes of protein extracts were adjusted to 1.5 mL with homogenizing buffer including protease inhibitors and a 20µl aliquot was collected for Western blotting ("total fraction"). Naked Sepharose beads (200µL per protein extract) were incubated with protein extracts and agitated for 2 hours at 4°C. After centrifugation (1300g, 3 min, 4°C), supernatants were mixed to 200µL of p9 beads or naked beads (negative control) and agitated for 2.5 hours at 4°C. After centrifugation (1300g, 3min, 4°C), the supernatants (30µL) were collected for Western blotting ("unbound fraction") and the pellets of p9 beads were washed four times with 5 mL of washing buffer (Tris-HCl pH 7.4, 5mM NaF, 250 mM NaCl, 5mM EDTA, 5mM EGTA, 0.1% Nonidet P-40) with protease inhibitors. The proteins were eluted with 150 µL of Laemmli buffer and heated at 85°C for 5min.

2.5. Immunoblotting

Proteins were separated by 12% SDS-PAGE and transferred to Hybond C membranes (GE Healthcare). Membranes were probed with antibodies to: CDK1 (mouse monoclonal, MS-110-PO, Interchim), Cyclin B2 (gift from T. Lorca, CRBM, Montpellier, France; rabbit polyclonal) and MCM4 (both gifts from M. Méchali, IGH, Montpellier, France, rabbit polyclonal).

2.6. Sample preparation for mass spectrometry analysis

Eluted proteins were resolved on a 4-12% Criterion™ XT Bis-Tris gradient gel (Bio-Rad), and stained with SYPRO Ruby (Bio-Rad). Images were acquired on a Geliance CCD-based bioimaging system (PerkinElmer).

2.7. LC-MS/MS analysis

The entire protein profile of each lane on SDS-PAGE was sliced from the gel into 16 bands using a gel excision Lanepicker™ (The Gel Company). Gel slices were deposited into 96-well

plates. In-gel protein digestion was performed by a MassPrep™ liquid handling station (Micromass), using sequencing-grade modified trypsin (Promega). Peptide extracts were dried using a SpeedVac™. Peptide extracts were separated by online reversed-phase (RP) nanoscale capillary liquid chromatography (nanoLC) and analyzed by ES MS/MS. Analyses were performed on a Thermo Surveyor MS pump connected to an LTQ linear ion trap mass spectrometer (Thermo Electron, San Jose, CA) equipped with a nanoelectrospray ion source (Thermo Electron, San Jose, CA). Peptide separation took place within a PicoFrit column BioBasic C18, 10 cm x 0.075 mm internal diameter (New Objective, Woburn, MA) with a linear gradient from 2 to 50% solvent B (acetonitrile, 0.1% formic acid) in 30 min, at 200 nL/min. Mass spectra were acquired using data dependent acquisition mode (Xcalibur software, version 2.0). Each full-scan mass spectrum (400 to 2000 m/z) was followed by collision-induced dissociation of the seven most intense ions. The dynamic exclusion function was enabled (30 s exclusion), and the relative collisional fragmentation energy was set to 35%.

2.8. *Interpretation of Tandem-MS Spectra*

The RAW files generated from MS/MS spectra were uploaded to the MASCOT search engine (Matrix Science, London, UK; version 2.2.0) for protein identifications. The parameters for database searching were as follows: (I) Protein database: Uniref_100, (II) Taxonomy: Xenopus laevis [TaxID: 8355, 15 599 entries], (III) Trypsin digestion with up to two missed cleavage sites, (IV) Fragment and parent ion mass tolerance were 0.5 Da and 2.0 Da respectively, (V) Iodoacetamide derivative of cysteine as a fixed modification and oxidation of methionine as a variable modification.

2.9. Criteria for protein identification

Scaffold (version 03_00_01, Proteome Software Inc., Portland, OR) was used to validate MS/MS based peptide and protein identifications, and to provide confidence level (% probability) of the identification. Peptide identifications were accepted if they could be established at greater than 95.0% probability by the PeptideProphet algorithm (Keller *et al.*, 2002). Protein identifications were accepted if they could be established at greater than 95.0% probability and contained at least 2 distinct peptides. Protein probabilities were assigned by the ProteinProphet algorithm (Nesvizhskii *et al.*, 2003). Proteins containing similar peptides

that could not be differentiated based on MS/MS analysis alone were grouped to satisfy the principles of parsimony. A Scaffold 3 report is provided as Supporting Information. This file can be accessed with a free viewer available from Proteome Software, Inc. website (http://www.proteomesoftware.com). This file contains all the spectral information, including the accession number for each protein sequence, Mascot scores, protein sequence coverage and amino acid residues modifications, statistical probability modeling, and spectral counting.

3. Results

We have applied two different affinity-based approaches to identify proteins bound to CDK1. The first approach is a classical CDK1 pull-down using an anti-CDK1 antibody (Krasinska et al. 2008), whereas the second is based on CDK1 precipitation via p9 beads (Patra and Dunphy, 1996). MS analysis was used to identify CDK1-associated proteins in M-phase, when the kinase is fully active, and during its inactivation upon M-phase exit. Experiments were repeated several times to establish the method. Below, we present data from single experiments obtained using IP and p9 purifications according to the final satisfactory procedure described in Materials & Methods section. Scaffold software was used to merge the identifications, validate the peptides and proteins hits and discriminate homologous proteins (150 unique proteins, 8866 spectra, 0.1% protein false discovery rate (FDR), see Supplementary file Protein IDs. SF3)

3.1. CDK1 immunoprecipitation

As shown in Fig. 1a, the protein markers (Mcm4 and cyclin B2) confirm MII exit. CDK1 immunoprecipitations were performed on extracts from MII-arrested eggs (T0) and activated eggs (7 minutes after activation, T7). A negative IP control with naked beads instead of anti-CDK1-coupled beads was performed. To assess the yield during the stages of purification, aliquots of total egg extract (total), unbound fraction (unbound) and proteins bound to the beads (bound) were taken for Western blot analysis. CDK1 was almost completely depleted from extracts (compare unbound and bound fractions from IP T0 and T7 in Fig. 1B). To verify if this approach also enables CDK1-interacting proteins to be precipitated, we assessed the presence of Cyclin B2. As expected, Cyclin B2 was also depleted and found in bead-bound fractions. We observed a clear decrease in cyclin B2 abundance between T0 and T7 extracts, confirming activation of eggs. No signal for CDK1 and Cyclin B2 was found in

negative-control bound fractions, indicating that protein interactions were specific. These results showed that both CDK1 and CDK1-associated proteins were efficiently depleted.

SYPRO Ruby-stained gel containing all four bound fractions (M-phase, M-phase exit and their respective negative controls) showed quantitative and qualitative differences (Fig. 1C). Control samples contained much less protein than immunoprecipitation samples, indicating that proteins interacting with CDK1 are abundant and that only few proteins interact nonspecifically with naked beads. Differences between bound fractions of M-phase-arrested and activated extracts were also visible, suggesting that partners of CDK1 change upon M-phase exit. To identify CDK1 partners, protein bands corresponding to the entire gel were excised and analyzed by LC-MS/MS. We identified 30 proteins during M-phase (Table 1) and 42 during M-phase exit (Table 2). A total of 23 proteins were common to both samples. As expected, the major biological process that stands out for CDK1-associated proteins is cell cycle progression (Fig. 2). A few other purified proteins are involved in DNA/RNA metabolism, cytoskeleton/vesicle transport, fertilization for the M-phase sample. Most importantly for the validity of the analysis, the two isoforms of CDK1, Cdc2-A and Cdc2-B, were identified in both samples. Moreover, among the 21 proteins common to both samples, four are involved in cell division, and two, Cyclins B2 and B4, are known regulatory subunits of CDK1. The two other cell cycle proteins common for M-phase and M-phase exit samples, are ERK2 (mitogen activated protein kinase 1) and calcineurin A (a serine/threonine protein phosphatase). Another category of proteins shared between M-phase and M-phase exit are chaperones belonging to T-complex protein1 (Tcp1) family and heat-shock proteins (A8 and D1).

Among proteins specifically interacting with M-phase CDK1, three are egg envelope components (XlZPA, egg envelope glycoprotein and component ZPAX). M-phase exit-specific CDK1-interactors are mainly involved in metabolism (7 out of 19) and this group apparently increases upon CDK1 inactivation. Among them, two are involved in proteolysis (arginyl aminopeptidase and LOC431925 protein). Interestingly, Septin 9 found in this group is potentially involved in late mitosis and cytokinesis (Bi et al., 1998; Cao et al., 2009; Nguyen et al., 2000; Spiliotis et al., 2005). The other proteins found exclusively during M-phase exit are involved in protein folding (a member of Tcp1 family), cytoskeleton/vesicle transport (2 proteins), DNA/RNA metabolism (2 proteins) and other functions (5 proteins). As expected, fertilization-specific proteins were missing in CDK1 complexes following oocyte activation.

3.2 Affinity purification with p9-beads

As shown in Fig. 3A, protein markers confirmed egg activation. As in CDK1 IP, p9 precipitation was performed on extracts from MII (T0) eggs, and eggs 7 min after activation (T7). CDK1 was almost completely depleted from egg extracts (compare unbound and bound fractions from p9 T0 and T7 in Fig. 3B). We also searched for Cyclin B2 in the different fractions to test whether this method allows co-precipitation of CDK1 partners. As expected, Cyclin B2 was depleted from the extract, and was found in the bound fraction of the T0 extract. We did not detect Cyclin B2 in the bound fraction of the T7 extract, due to its almost complete degradation at this time point. No signals for CDK1 and Cyclin B2 were detected in the negative control bound fractions, indicating that protein interactions were specific. These results showed that p9 precipitation depleted both CDK1 and its associated proteins.

The staining of the gel containing all four bound fractions showed fewer differences between samples than in IP experiments (Figs. 1C and 3C). Nineteen proteins were identified during M-phase (Table 3) and 37 during M-phase exit (Table 4). Sixteen proteins were common for the two samples. As in IP, p9 precipitation allowed us to identify more proteins in activated oocytes compared to MII-arrested ones (Fig. 3C). A functional classification indicates that the proteins identified are mainly involved in cell cycle, folding (heat shock proteins 70 kDa), metabolism (L-isoaspartate O-methyltransferase and XlGst) and DNA/RNA metabolism (Nif3-like protein 1, Ribosomal protein S30, Double-stranded RNA-binding protein A). Remaining proteins are involved in cytoskeleton/vesicle transport (Cofilin-1-A) and other functions (Traf2 and Nck-interacting protein kinase, Peroxiredoxin-2, Galectin-VIIa). As expected, p9 beads precipitated two isoforms of CDK1, Cdc2-A and Cdc2-B, next to CDK2 (represented by a single peptide, indicating a low amount; see Tables 3 and 4) in both samples showing that other identified proteins may be partners of either Cdc2-A or Cdc2-B subunit, and/or of CDK2. Identification of Cyclins B2 and B4 confirmed the presence of CDK1-associated proteins in p9 samples. Concerning specific M-phase proteins in p9-precipitates, two are B-type Cyclins (B1 and B5) and one is involved in cell adhesion (Junction plakoglobin). Proteins specific for M-phase exit (Table 4) are mainly involved in metabolism (6 out of 21), DNA/RNA metabolism (6 proteins), protein folding (3), and other functions (6).

3.3 Comparative analysis of the two approaches

Among all proteins co-purified with CDK1 and identified by these two approaches, six were common for all samples: Cdc2A, Cdc2B, Cyclin B2, Cyclin B4, Peroxiredoxin-2 and Heat shock protein A8 (Fig. 5). The presence of two CDK1 isoforms and two B-type Cyclins (B2 and B4) in all samples confirms that CDK1 partners could indeed be present among other identified proteins. None of the proteins was exclusively present in M-phase samples, whereas two proteins involved in metabolism were specific for M-phase exit samples: pyruvate kinase and the α subunit of ATP synthase (Fig. 5). The presence of pyruvate kinase and the α subunit of ATP synthase in M-phase exit samples obtained by two methods argue for their real association with CDK1.

4. Discussion

4.1. Validation of the proteomic screen

Our mass spectrometry analysis of CDK1 co-IPed proteins was supplemented by analysis of p9-precipitates. Large-scale proteomic screens often give rise to false-positive interactions (e.g. Trinkle-Mulcahy et al. 2008). The analysis of p9-precipitated proteins focused on verification of major CDK1 partners found by IP, as p9 beads also precipitate p9-specific partners, which may not be associated with either CDK1 or CDK2. Despite this shortcoming that makes the p9 precipitation less stringent for CDK1 partners than CDK1 IP, p9-beads are widely used to precipitate CDK1 in *Xenopus* oocytes, for instance to measure CDK1 activity (Patra and Dunphy, 1996). In both cases two CDK1 isoforms, Cdc2-A and Cdc2-B, and CDK1 partners, cyclins B2 and B4, were identified. CDK1 was used as a positive control in a proteomic screen using HeLa cells and cyclins B were also identified as CDK1 interactors as expected (Fig. S5(B) in Hutchins at al. 2010; www.mitocheck.org). In addition, in our screen the number of identified peptides of two cyclins B diminished in M-phase exit samples concomitant with their advanced degradation. The successful identification of remaining Cyclins B2 and B4 in activated oocytes (both with IP and p9 precipitation) demonstrates the relative sensitivity of the method used here to purify CDK1 protein complexes. These data auto-validated our screen and confirmed that we efficiently co-IPed partners of CDK1 (Cdc2-A or Cdc2-B) complexes. The absence of CDK2, the closest CDK to CDK1 in oocytes, in the IP further confirmed the specificity of this method. Thus the combination of methods used was appropriate for the purification of complexes containing CDK1 in both states: fully active and being inactivated CDK1 complex purification.

Among other identified proteins only two were common for all samples (Peroxiredoxin-2 and Heat shock protein A8) and two (pyruvate kinase and the α subunit of ATP synthase) specific for M-phase exit samples and detected by both approaches. All these proteins were found often as contaminants in other proteomic analyses (Trinkle-Mulcahy et al. 2008). However, the absence of these proteins in our control argues for their true association with CDK1 (see Tables 1-4). As p9 precipitation is a method that enables the purification of CDK1, CDK2 and p9 partners, specific interactors of CDK1 are diluted among all co-precipitated proteins. As a consequence, their identification by mass spectrometry analysis could be impaired explaining why the number of overlapping proteins between the two methods is low. Another explanation could rely on differences in experimental conditions, more stringent for p9 precipitations than for IP, decreasing the number of proteins purified on p9 beads. Nevertheless, we managed to identify molecules engaged in CDK1 complexes at two studied states of activity and the major components common for the two methods.

4. 2. CDK1 partners specifically present during M-phase exit

Our proteomic analysis revealed the presence of two proteins specifically detected during M-phase exit: pyruvate kinase and the α subunit of ATP synthase, both involved in cellular energy metabolism. Pyruvate kinase PKM2 was also identified as a CDK1 partner in human cells, but without indication of a potential cell cycle-dependent association (Hutchins et al. 2010; www.mitocheck.org). An interaction between CDK1 and the α subunit of ATP synthase has never been demonstrated and its significance remains unclear considering their functions and subcellular localization. Pyruvate kinase and ATP synthase could associate with inactive CDK1 or could be attached to a common support fixing CDK1 during its inactivation for example on cytoskeletal elements, as CDK1 associates with the spindle and its inactivation requires a functional spindle (Kubiak et al. 1993; Thibier et al. 1997). The association between CDK1 and metabolic enzymes involved in cell cycle progression is an attractive hypothesis. For instance, 6-phosphofructo-2-kinase (PFKFB3) and fructose 2,6-bisphosphate activate CDK1 to phosphorylate p27 in HeLa lysates, indicating that these proteins may have direct allosteric effects activating CDK1 (Yalcin et al. 2009). The link between ATP cycle and CDK1 inactivation is also obvious in the light of the requirement of ATP for cyclin B polyubiquitination and M-phase exit (Miniowitz-Shemtov et al. 2010).

Interestingly, Hutchins and collaborators (2010) also found, besides pyruvate kinase, a number of metabolic enzymes associated with CDK1 in HeLa cells (e.g. carbonic anhydrase CA2, carbamoyl-phosphate synthase 1 CPS1, tRNA (cytosine-5-)-methyltransferase NSUN2, phosphoglycerate kinase 1 PGK1, 3-phosphoglycerate dehydrogenase PHGDH, thymidine phosphorylase TYMP; www.mitocheck.org).

Among potential CDK1 partners specifically present during M-phase exit following CDK1 IP, two are known to be involved in cytoskeleton functions: dynein, the microtubule motor protein (Burakov and Nadezhdina, 2006) and septin 9, a GTP binding protein involved in microtubule and actin function (Cao *et al.*, 2009). This is also in agreement with results obtained by Hutchins and colleagues (2010), who identified a number of cytoskeletal proteins associated with human CDK1 (e.g. ezrin EZR, actin-related protein 3 homolog ACTR3, actin binding protein coronin CORO1C, dynactin 1 DCTN1, Cytoplasmic dynein 1 heavy chain 1 DYNC1H1, non-erythrocytic spectrin SPTBN2; www.mitocheck.org). CDK1/cyclin B is localized on the spindle in mitosis and meiosis, where it regulates spindle formation and maintenance (Brunet and Maro, 2005; Huo et al., 2005; Nakamura et al., 2005). Moreover, an intact spindle is necessary for cyclin B degradation and CDK1 inactivation (Kubiak et al. 1993; Thibier et al. 1997). Thus, interactions between CDK1 and microtubule-interacting proteins seem of great importance for spindle maintenance and for correct localization of CDK1 own residual activity. The presence of actin-related proteins both in our screen and by Hutchins et al. (2010) argues the need for a serious analysis of CDK1-actin cytoskeleton interactions.

4.3. CDK1 partners common for M phase and M-phase exit

Among common putative partners of CDK1 identified by our two approaches, the molecular chaperone HspA8, a member of Hsp70 family, seems to be particularly interesting. Hsp70 colocalizes with CDK1 on the meiotic spindle of sea urchin oocytes (Geraci *et al.*, 2003). A member of the Hsp70 family (Hsp70-2) is a molecular chaperone of CDK1 involved in CDK1/cyclin B1 complex formation, and essential for the cell cycle in spermatogenesis (Dix *et al.*, 1996; Zhu *et al.*, 1997). Interestingly, we did not find any members of the Hsp90 family, known as Mos-specific chaperone in *Xenopus laevis* oocytes (Fisher *et al*. 2000). Taken together, these results show a clear molecular link between the Hsp70 family and CDK1, confirmed by our proteomic screen.

The other common protein for all samples is Peroxiredoxin-2, a protein involved in cell redox homeostasis (Hofmann *et al.*, 2002). Two members of Peroxiredoxin family (Prx family) including Prx-2 are phosphorylated *in vitro* by CDK1 (Chang *et al.*, 2002). *In vivo* phosphorylation of Prx-1 on Thr90 occurs only during mitosis when CDK1 is active. A proteomic screen performed in bovine oocytes also revealed that Prx-2 is phosphorylated during oocyte maturation via CDK1 or MAPK (Bhojwani *et al.*, 2006). CDK1-mediated phosphorylation at Thr90 of Prx-1 leads to decrease of its activity (Chang *et al.*, 2002). The significance of Prx-1 inactivation and consequently of H_2O_2 increase on the M-phase progression remains unclear. However, one putative target of H_2O_2 could be the Cdc25C phosphatase, a major CDK1 activator (Morgan, 1995; Perdiguero and Nebreda, 2004; Wang *et al.*, 2007). Cdc25C activity requires reducing agents, and oxidative stress induces its degradation (Savitsky and Finkel, 2002). The CDK1-Prx-2 interaction suggested by our screen could lead to CDK1-dependent inhibitory phosphorylation of Prx-2, and consequently an increase in H_2O_2 concentration. This oxidative stress could participate in Cdc25C inactivation, and in turn CDK1 inactivation. As peroxiredoxins often appear often as contaminants in proteomic screens (Trinkle-Mulcahy et al. 2008), the potential association between Prx-2 and CDK1 will have to be carefully examined.

Among common potential CDK1 partners during M-phase and M-phase exit in both methods used in our study, several were involved in cytoskeletal functions. In the IP experiments kinectin, a membrane anchor for kinesin (Kumar *et al.*, 1995), was especially abundant. Copin, a calcium-dependent membrane binding protein involved in membrane trafficking (Creutz *et al.*, 1998) was also identified during M-phase and M-phase exit by IP. On the other hand, cofilin 1-A (Bernstein and Bamburg, 2010) was identified in both p9 samples (Tables 3 and 4). A member of cofilin family was already reported as a substrate of CDK1 and its phosphorylation is involved in the functionality of inositol (1,4,5)-trisphosphate receptors in starfish oocytes (Santella *et al.*, 2003). Copin A knockout in *Dictyostelium* leads to the formation of multinucleated cells (Damer *et al.*, 2007) and cofilin localizes at the contractile ring, suggesting their involvement in cytokinesis (Nagaoka *et al.*, 1995). Together with the identification of septin 9 during M-phase exit by IP, these results suggest interplay between CDK1 and cytokinesis. Other proteins linking CDK1 and cytoskeleton are members of TCP1 complex family, identified in two IP samples. They are involved in tubulin folding (Brown *et al.*, 1996) and colocalizes with CDK1 at the mitotic spindle in sea urchin embryos (Agueli *et al.*, 2001). All these results suggest that CDK1 is cytoskeleton-anchored.

Among common putative CDK1 partners during M-phase and M-phase exit present only in IP samples, two are involved in cell cycle regulation: calcineurin A and ERK2. Calcineurin is a highly conserved phosphatase composed of a catalytic subunit, calcineurin A and a regulatory one, calcineurin B (Rusnak and Mertz, 2000). Calcineurin is required for CSF release during MII exit in *Xenopus* oocytes via dephosphorylation of Apc3 and Cdc20 contributing to APC/C activation and cyclin B2 degradation (Chung and Chen, 2003; Mochida and Hunt, 2007; Nishiyama et al., 2007; Yudkovsky et al., 2000). Calcineurin is also required for completion of meiosis in *Drosophila* oocytes (Takeo *et al.*, 2010). The association between calcineurin A and CDK1 that we found may suggest that these two proteins regulate each other, or are linked by a common support (e.g. the cytoskeleton).

ERK2 MAP kinase is involved in CDK1 activation during oocyte maturation (Castro *et al.*, 2001). The ERK2 pathway catalyzes the inhibitory phosphorylation of Myt1 kinase, responsible for the inhibitory phosphorylation of CDK1 on Thr14 and Tyr 15 (Mueller *et al.*, 1995), and is required for CDK1 activation. ERK2 is also involved in activation of Cdc25C at the G2/M transition (Wang *et al.*, 2007) and Cdc25 is essential for CSF arrest (Lorca *et al.*, 2010). A clear feedback links ERK2 and CDK1 in meiosis (Abrieu *et al.*, 2001), which changes during embryonic mitosis (Bazile *et al.* 2007). Thus, CDK1 and ERK2 are functionally related especially during meiosis. However, until now no physical association between these proteins has been shown.

4.4. Different CDK1 complexes with potentially different functions

Each of two CDK1 isoforms identified in this study (Cdc2-A and B) may be associated with different types of partners. The nature of the cyclin associated with CDK1 is essential for the substrate specificity of CDK1. Upon M-phase exit the timing of cyclin degradation is sequential (Hochegger *et al.*, 2001). Thus, different CDK1 complexes may exert various functions according to the type of cyclin they harbour (Gong and Ferrell, 2010; Kõivomägi et al. 2011). The spectrum of different CDK1 complexes can be enlarged by association with other partners identified in the current study.

4.5. Conclusions

In this paper we have shown that CDK1 interacts with different proteins depending on the cell cycle stage (namely upon MII-arrest and oocytes activation). Our results show the

necessity to study individually CDK1-other proteins associations to fully understand the regulation of this major cell cycle kinase. It also completes information on potential CDK1 associated proteins previously obtained in much larger screen of protein complexes involved in mitotic regulation by Hutchins et al. (2010) in human cells. Our dynamic approach points the necessity to analyse the evolution of protein complexes to better understand cell cycle regulation and especially the mitotic progression.

Acknowledgements

We are grateful to Laurent Meijer and Olivier Lozach (Roscoff, France) for p9 beads, Thierry Lorca (Montpellier, France) for the gift of a large quantity of precipitating *Xl*CDK1 antibody , Marcel Méchali (Montpellier, France) for MCM4 antibody and James R. Hutchins (Montpellier, France) for valuable discussions and critical reading of the manuscript. The authors were supported by grants from Ligue Contre le Cancer and Association pour la Recherche contre le Cancer to JZK. GM was a recipient of a fellowship from the French Ministère de la Recherche et de l'Enseignement supérieur and MED from the Lebanese Government.

References

Abrieu, A., Doree, M. and Fisher, D. (2001). The interplay between cyclin-B-Cdc2 kinase (MPF) and MAP kinase during maturation of oocytes. *J Cell Sci* 114, 257-67.

Agueli, C., Geraci, F., Giudice, G., Chimenti, L., Cascino, D. and Sconzo, G. (2001). A constitutive 70 kDa heat-shock protein is localized on the fibres of spindles and asters at metaphase in an ATP-dependent manner: a new chaperone role is proposed. *Biochem J* 360, 413-9.

Archambault, V., Li, C. X., Tackett, A. J., Wasch, R., Chait, B. T., Rout, M. P. and Cross, F. R. (2003). Genetic and biochemical evaluation of the importance of Cdc6 in regulating mitotic exit. *Mol Biol Cell* 14, 4592-604.

Bazile F, Pascal A, Karaiskou A, Chesnel F, Kubiak JZ. (2007). Absence of reciprocal feedback between MPF and ERK2 MAP kinase in mitotic Xenopus laevis embryo cell-free extract. Cell Cycle 6, 489-96.

Bazile F, Gagné JP, Mercier G, Lo KS, Pascal A, Vasilescu J, Figeys D, Poirier GG, Kubiak* JZ, Chesnel F. (2008). Differential Proteomic Screen To Evidence Proteins Ubiquitinated upon Mitotic Exit in Cell-Free Extract of Xenopus laevis Embryos. J Proteome Res. 7(11), 4701-4714.

Bernstein, B. W. and Bamburg, J. R. (2010). ADF/cofilin: a functional node in cell biology. *Trends Cell Biol* 20, 187-95.

Bhojwani, M., Rudolph, E., Kanitz, W., Zuehlke, H., Schneider, F. and Tomek, W. (2006). Molecular analysis of maturation processes by protein and phosphoprotein profiling during in vitro maturation of bovine oocytes: a proteomic approach. *Cloning Stem Cells* 8, 259-74.

Bi, E., Maddox, P., Lew, D. J., Salmon, E. D., McMillan, J. N., Yeh, E. and Pringle, J. R. (1998). Involvement of an actomyosin contractile ring in Saccharomyces cerevisiae cytokinesis. *J Cell Biol* 142, 1301-12.

Brown, C. R., Doxsey, S. J., Hong-Brown, L. Q., Martin, R. L. and Welch, W. J. (1996). Molecular chaperones and the centrosome. A role for TCP-1 in microtubule nucleation. *J Biol Chem* 271, 824-32.

Brunet, S. and Maro, B. (2005). Cytoskeleton and cell cycle control during meiotic maturation of the mouse oocyte: integrating time and space. *Reproduction* 130, 801-11.

Bueno, A and Rusell P. (1992). Dual functions of *CDC6*: a yeast protein required for DNA replication also inhibits nuclear division. The EMBO J. 11, 2167-76.

Burakov, A. V. and Nadezhdina, E. S. (2006). [Dynein and dynactin as organizers of the system of cell microtubules]. *Ontogenez* 37, 323-39.

Calzada, A., Sacristan, M., Sanchez, E. and Bueno, A. (2001). Cdc6 cooperates with Sic1 and Hct1 to inactivate mitotic cyclin-dependent kinases. *Nature* 412, 355-8.

Cao, L., Yu, W., Wu, Y. and Yu, L. (2009). The evolution, complex structures and function of septin proteins. *Cell Mol Life Sci* 66, 3309-23.

Castro, A., Peter, M., Lorca, T. and Mandart, E. (2001). c-Mos and cyclin B/cdc2 connections during Xenopus oocyte maturation. *Biol Cell* 93, 15-25.

Chang, T. S., Jeong, W., Choi, S. Y., Yu, S., Kang, S. W. and Rhee, S. G. (2002). Regulation of peroxiredoxin I activity by Cdc2-mediated phosphorylation. *J Biol Chem* 277, 25370-6.

Chen, J., Jackson, P. K., Kirschner, M. W. and Dutta, A. (1995). Separate domains of p21 involved in the inhibition of Cdk kinase and PCNA. *Nature* 374, 386-8.

Chesnel, F., Bazile, F., Pascal, A. and Kubiak, J. Z. (2006). Cyclin B dissociation from CDK1 precedes its degradation upon MPF inactivation in mitotic extracts of Xenopus laevis embryos. *Cell Cycle* 5, 1687-98.

Chesnel, F., Bazile, F., Pascal, A. and Kubiak, J. Z. (2007). Cyclin B2/cyclin-dependent kinase1 dissociation precedes CDK1 Thr-161 dephosphorylation upon M-phase promoting factor inactivation in Xenopus laevis cell-free extract. *Int J Dev Biol* 51, 297-305.

Chung, E. and Chen, R. H. (2003). Phosphorylation of Cdc20 is required for its inhibition by the spindle checkpoint. *Nat Cell Biol* 5, 748-53.

Creutz, C. E., Tomsig, J. L., Snyder, S. L., Gautier, M. C., Skouri, F., Beisson, J. and Cohen, J. (1998). The copines, a novel class of C2 domain-containing, calcium-dependent, phospholipid-binding proteins conserved from Paramecium to humans. *J Biol Chem* 273, 1393-402.

Damer, C. K., Bayeva, M., Kim, P. S., Ho, L. K., Eberhardt, E. S., Socec, C. I., Lee, J. S., Bruce, E. A., Goldman-Yassen, A. E. and Naliboff, L. C. (2007). Copine A is required for cytokinesis, contractile vacuole function, and development in Dictyostelium. *Eukaryot Cell* 6, 430-42.

De Clercq, A. and Inze, D. (2006). Cyclin-dependent kinase inhibitors in yeast, animals, and plants: a functional comparison. *Crit Rev Biochem Mol Biol* 41, 293-313.

Dix, D. J., Allen, J. W., Collins, B. W., Mori, C., Nakamura, N., Poorman-Allen, P., Goulding, E. H. and Eddy, E. M. (1996). Targeted gene disruption of Hsp70-2 results in failed meiosis, germ cell apoptosis, and male infertility. *Proc Natl Acad Sci U S A* 93, 3264-8.

Elsasser, S., Lou, F., Wang, B., Campbell, J. L. and Jong, A. (1996). Interaction between yeast Cdc6 protein and B-type cyclin/Cdc28 kinases. *Mol Biol Cell* 7, 1723-35.

Fisher DL, Mandart E, Dorée M. (2000). Hsp90 is required for c-Mos activation and biphasic MAP kinase activation in Xenopus oocytes. EMBO J. 19, 1516-24.

Gautier, J., Norbury, C., Lohka, M., Nurse, P. and Maller, J. (1988). Purified maturation-promoting factor contains the product of a Xenopus homolog of the fission yeast cell cycle control gene cdc2+. *Cell* 54, 433-9.

Geraci, F., Agueli, C., Giudice, G. and Sconzo, G. (2003). Localization of HSP70, Cdc2, and cyclin B in sea urchin oocytes in non-stressed conditions. *Biochem Biophys Res Commun* 310, 748-53.

Gong, D. and Ferrell, J. E., Jr. (2010). The roles of cyclin A2, b1, and b2 in early and late mitotic events. *Mol Biol Cell* 21, 3149-61.

Hochegger, H., Klotzbucher, A., Kirk, J., Howell, M., le Guellec, K., Fletcher, K., Duncan, T., Sohail, M. and Hunt, T. (2001). New B-type cyclin synthesis is required between meiosis I and II during Xenopus oocyte maturation. *Development* 128, 3795-807.

Hofmann, B., Hecht, H. J. and Flohe, L. (2002). Peroxiredoxins. *Biol Chem* 383, 347-64.

Huo, L. J., Yu, L. Z., Liang, C. G., Fan, H. Y., Chen, D. Y. and Sun, Q. Y. (2005). Cell-cycle-dependent subcellular localization of cyclin B1, phosphorylated cyclin B1 and p34cdc2 during oocyte meiotic maturation and fertilization in mouse. *Zygote* 13, 45-53.

Hutchins JR, Toyoda Y, Hegemann B, Poser I, Hériché JK, Sykora MM, Augsburg M, Hudecz O, Buschhorn BA, Bulkescher J, Conrad C, Comartin D, Schleiffer A, Sarov M, Pozniakovsky A, Slabicki MM, Schloissnig S, Steinmacher I, Leuschner M, Ssykor A, Lawo S, Pelletier L, Stark H, Nasmyth K, Ellenberg J, Durbin R, Buchholz F, Mechtler K, Hyman AA, Peters JM. (2010). Systematic analysis of human protein complexes identifies chromosome segregation proteins. Science 328, 593-9.

Keller, A., Nesvizhskii, A. I., Kolker, E. and Aebersold, R. (2002). Empirical statistical model to estimate the accuracy of peptide identifications made by MS/MS and database search. *Anal Chem* 74, 5383-92.

Kõivomägi M, Valk E, Venta R, Iofik A, Lepiku M, Morgan DO, Loog M. (2011). Dynamics of Cdk1 substrate specificity during the cell cycle. Mol Cell. 42, 610-23.

Krasinska L, Besnard E, Cot E, Dohet C, Méchali M, Lemaitre JM, Fisher D. (2008). Cdk1 and Cdk2 activity levels determine the efficiency of replication origin firing in Xenopus. EMBO J. 27, 758-69.

Kubiak JZ, Weber M, de Pennart H, Winston NJ, Maro B. (1993). The metaphase II arrest in mouse oocytes is controlled through microtubule-dependent destruction of cyclin B in the presence of CSF. EMBO J. 12, 3773-8.

Kubiak J.Z. & El Dika M. (2011). Canonical and alternative pathways in Cyclin-Dependent Kinase 1/cyclin B inactivation upon M-phase exit in *Xenopus laevis* cell-free extracts. Enzyme Res. (in press).

Kumar, J., Yu, H. and Sheetz, M. P. (1995). Kinectin, an essential anchor for kinesin-driven vesicle motility. *Science* 267, 1834-7.

Labbe, J. C., Capony, J. P., Caput, D., Cavadore, J. C., Derancourt, J., Kaghad, M., Lelias, J. M., Picard, A. and Doree, M. (1989). MPF from starfish oocytes at first meiotic metaphase is a heterodimer containing one molecule of cdc2 and one molecule of cyclin B. *EMBO J* 8, 3053-8.

Laemmli, U. K. (1970). Cleavage of structural proteins during the assembly of the head of bacteriophage T4. *Nature* 227, 680-5.

Lohka, M. J., Hayes, M. K. and Maller, J. L. (1988). Purification of maturation-promoting factor, an intracellular regulator of early mitotic events. *Proc Natl Acad Sci U S A* 85, 3009-13.

Lorca, T., Bernis, C., Vigneron, S., Burgess, A., Brioudes, E., Labbe, J. C. and Castro, A. (2010). Constant regulation of both the MPF amplification loop and the Greatwall-PP2A pathway is required for metaphase II arrest and correct entry into the first embryonic cell cycle. *J Cell Sci* 123, 2281-91.

Masui, Y. and Markert, C. L. (1971). Cytoplasmic control of nuclear behavior during meiotic maturation of frog oocytes. *J Exp Zool* 177, 129-45.

McConnell, B. B., Gregory, F. J., Stott, F. J., Hara, E. and Peters, G. (1999). Induced expression of p16(INK4a) inhibits both CDK4- and CDK2-associated kinase activity by reassortment of cyclin-CDK-inhibitor complexes. *Mol Cell Biol* 19, 1981-9.

Miniowitz-Shemtov S, Teichner A, Sitry-Shevah D, Hershko A. (2010). ATP is required for the release of the anaphase-promoting complex/cyclosome from inhibition by the mitotic checkpoint. Proc Natl Acad Sci U S A. 107, 5351-6.

Mochida, S. and Hunt, T. (2007). Calcineurin is required to release Xenopus egg extracts from meiotic M phase. *Nature* 449, 336-40.

Morgan, D. O. (1995). Principles of CDK regulation. *Nature* 374, 131-4.

Mueller, P. R., Coleman, T. R., Kumagai, A. and Dunphy, W. G. (1995). Myt1: a membrane-associated inhibitory kinase that phosphorylates Cdc2 on both threonine-14 and tyrosine-15. *Science* 270, 86-90.

Nagaoka, R., Abe, H., Kusano, K. and Obinata, T. (1995). Concentration of cofilin, a small actin-binding protein, at the cleavage furrow during cytokinesis. *Cell Motil Cytoskeleton* 30, 1-7.

Nakamura, N., Tokumoto, T., Ueno, S. and Iwao, Y. (2005). The cytoskeleton-dependent localization of cdc2/cyclin B in blastomere cortex during Xenopus embryonic cell cycle. *Mol Reprod Dev* 72, 336-45.

Nesvizhskii, A. I., Keller, A., Kolker, E. and Aebersold, R. (2003). A statistical model for identifying proteins by tandem mass spectrometry. *Anal Chem* 75, 4646-58.
Nguyen, T. Q., Sawa, H., Okano, H. and White, J. G. (2000). The C. elegans septin genes, unc-59 and unc-61, are required for normal postembryonic cytokineses and morphogenesis but have no essential function in embryogenesis. *J Cell Sci* 113 Pt 21, 3825-37.
Nishiyama, A., Tachibana, K., Igarashi, Y., Yasuda, H., Tanahashi, N., Tanaka, K., Ohsumi, K. and Kishimoto, T. (2000). A nonproteolytic function of the proteasome is required for the dissociation of Cdc2 and cyclin B at the end of M phase. *Genes Dev* 14, 2344-57.
Nishiyama, T., Yoshizaki, N., Kishimoto, T. and Ohsumi, K. (2007). Transient activation of calcineurin is essential to initiate embryonic development in Xenopus laevis. *Nature* 449, 341-5.
Parry, D., Mahony, D., Wills, K. and Lees, E. (1999). Cyclin D-CDK subunit arrangement is dependent on the availability of competing INK4 and p21 class inhibitors. *Mol Cell Biol* 19, 1775-83.
Patra, D. and Dunphy, W. G. (1996). Xe-p9, a Xenopus Suc1/Cks homolog, has multiple essential roles in cell cycle control. *Genes Dev* 10, 1503-15.
Riabowol, K., Draetta, G., Brizuela, L., Vandre, D. and Beach, D. (1989). The cdc2 kinase is a nuclear protein that is essential for mitosis in mammalian cells. *Cell* 57, 393-401.
Rusnak, F. and Mertz, P. (2000). Calcineurin: form and function. *Physiol Rev* 80, 1483-521.
Santella, L., Ercolano, E., Lim, D., Nusco, G. A. and Moccia, F. (2003). Activated M-phase-promoting factor (MPF) is exported from the nucleus of starfish oocytes to increase the sensitivity of the Ins(1,4,5)P3 receptors. *Biochem Soc Trans* 31, 79-82.
Savitsky, P. A. and Finkel, T. (2002). Redox regulation of Cdc25C. *J Biol Chem* 277, 20535-40.
Spiliotis, E. T., Kinoshita, M. and Nelson, W. J. (2005). A mitotic septin scaffold required for Mammalian chromosome congression and segregation. *Science* 307, 1781-5.
Takeo, S., Hawley, R. S. and Aigaki, T. (2010). Calcineurin and its regulation by Sra/RCAN is required for completion of meiosis in Drosophila. *Dev Biol* 344, 957-67.
Thibier C, De Smedt V, Poulhe R, Huchon D, Jessus C, Ozon R. (1997). In vivo regulation of cytostatic activity in Xenopus metaphase II-arrested oocytes. Dev Biol. 185, 55-66.
Trinkle-Mulcahy L, Boulon S, Lam YW, Urcia R, Boisvert FM, Vandermoere F, Morrice NA, Swift S, Rothbauer U, Leonhardt H, Lamond A. (2008). Identifying specific protein interaction partners using quantitative mass spectrometry and bead proteomes. J Cell Biol. 183, 223-39.
van Zon, W., Ogink, J., ter Riet, B., Medema, R. H., te Riele, H. and Wolthuis, R. M. (2010). The APC/C recruits cyclin B1-Cdk1-Cks in prometaphase before D box recognition to control mitotic exit. *J Cell Biol* 190, 587-602.
Vogel L, Baratte B, Détivaud L, Azzi L, Leopold P, Meijer L. (2002). Molecular cloning and characterisation of p15(CDK-BP), a novel CDK-binding protein. Biochim Biophys Acta. 1589, 219-31.
Wang, R., He, G., Nelman-Gonzalez, M., Ashorn, C. L., Gallick, G. E., Stukenberg, P. T., Kirschner, M. W. and Kuang, J. (2007). Regulation of Cdc25C by ERK-MAP kinases during the G2/M transition. *Cell* 128, 1119-32.
Yalcin A, Clem BF, Simmons A, Lane A, Nelson K, Clem AL, Brock E, Siow D, Wattenberg B, Telang S, Chesney J. (2009). Nuclear targeting of 6-phosphofructo-2-kinase (PFKFB3) increases proliferation via cyclin-dependent kinases. J Biol Chem. 284, 24223-32.
Yim H. & Erikson R.L. (2010). Cell division cycle 6, a mitotic substrate of polo-like kinase 1, regulates chromosomal segregation mediated by cyclin-dependent kinase 1 and separase. Proc Natl Acad Sci U S A. 107, 19742-7.
Yudkovsky, Y., Shteinberg, M., Listovsky, T., Brandeis, M. and Hershko, A. (2000). Phosphorylation of Cdc20/fizzy negatively regulates the mammalian cyclosome/APC in the mitotic checkpoint. *Biochem Biophys Res Commun* 271, 299-304.
Zhu, D., Dix, D. J. and Eddy, E. M. (1997). HSP70-2 is required for CDC2 kinase activity in meiosis I of mouse spermatocytes. *Development* 124, 3007-14.

Figure legends

Fig. 1. Co-immunoprecipitation of CDK1 and its partners during M-phase and M-phase exit. (A) Egg activation was checked by following Mcm4 phosphorylation status and Cyclin B2 (CycB2) abundance by immunoblotting of extracts of eggs taken 0, 3, 7, 9, 15, 30 min after calcium ionophore addition. (B) Co-immunoprecipitation of CDK1 and its partner (CycB2) during M-phase (T0) and M-phase exit (T7) was checked by following its presence either in protein fractions bound to beads (Bound) or in the non-retained fractions (Unbound). The presence of CDK1 and CycB2 was also checked in negative controls (C-, naked beads) in order to control the specificity of the interactions. (C) Comparative protein profiles of bound fraction of each samples: M-phase CDK1 IP (T0), its negative control (c- T0), M-phase exit CDK1 IP (T7) and its negative control (c- T7). Eluted proteins were resolved on SDS-PAGE and revealed with SYPRO Ruby staining.

Fig. 2. Distribution of protein functions based on Gene Ontology (GO) classification and bibliography of putative MPF interactors during M-phase (IP T0) and M-phase exit (IP T7) identified by CDK1 immunoprecipitation followed by MS analysis.

Fig. 3. Co-precipitation of CDK1 and its partners using p9 beads during M-phase and M-phase exit. (A) Egg activation was checked by following Mcm4 phosphorylation status and CycB2 abundance by immunoblotting extracts of eggs taken 0, 3, 7, 9, 15, 30 min after calcium ionophore addition. (B) Co-precipitation of CDK1 and its partner (CycB2) during M-phase (T0) and M-phase exit (T7) was checked by following its presence either in protein fractions bound to the beads (Bound) or in the non-retained fractions (Unbound). The presence of CDK1 and CycB2 was also checked in negative controls (C-, naked beads) in order to control the specificity of the interactions. (C) Comparative protein profiles of bound fraction of each samples: M-phase CDK1 p9 precipitation (T0), its negative control (c- T0), M-phase exit CDK1 p9 precipitation (T7) and its negative control (c- T7). Eluted proteins were resolved on SDS-PAGE and revealed with SYPRO Ruby staining.

Fig. 4. Distribution of protein functions based on Gene Ontology (GO) classification and bibliography of putative CDK1 interactors during M-phase (P9 T0) and M-phase exit (P9 T7) identified by CDK1 precipitation via p9 beads followed by MS analysis.

Fig. 5. Common putative CDK1 interactors between IP and p9 precipitation during M-phase and M-phase exit. (A) Six proteins are common between IP and p9 precipitation M-phase samples (Cdc2A, Cdc2B, CycB2, CycB4, HspA8 and peroxiredoxine-2). (B) Eight proteins are common between IP and p9 precipitation M-phase exit samples (Cdc2A, Cdc2B, CycB2, CycB4, HspA8, Peroxiredoxine-2, Pyruvate kinase and the alfa subunit of ATPase). (C) Six proteins are common between IP and p9 precipitation M-phase and M-phase exit samples (Cdc2A, Cdc2B, CycB2, CycB4, HspA8 and Peroxiredoxine-2).

Table 1. Potential interactors of CDK1 identified by mass spectrometry from CDK1 immunoprecipitation in metaphase II arrest *X. laevis* UFE

	Protein name	Accession Number	Molecular Weight (kDa)	Unique peptide c-T0	Unique peptide IP T0	Biological process
1	kinectin 1	Q08B03	97	0	12	Microtubule-based movement
2	Cell division control protein 2-A	P35567	35	0	11	Cell division
3	Heat Shock Protein A8	Q7ZTK6	71	1	9	ATP binding
4	Cyclin B2	Q6PA39	44	0	5	Cell division
5	Mitogen-activated protein kinase 1	P26696	41	0	4	Cell cycle
6	Cyclin B4	Q98TI3	44	0	4	Cell division
7	Egg cortical granule lectin	Q91719	34	0	4	Signal transduction
8	Transitional endoplasmic reticulum ATPase	P23787	89	0	3	Transport
9	Histone deacetylase 10	Q569T0	77	0	3	hydrolase activity
10	Cell division control protein 2-B	P24033	35	0	3	Cell division
11	T-complex protein 1 gamma subunit	P50143	61	0	3	Protein folding
12	Sorcin	A2VDA2	22	0	2	Calcium ion binding
13	RuvB like protein	Q0IH85	51	0	2	ATP binding
14	Heat shock protein d1	Q6IP60	62	0	2	Protein refolding
15	T-complex protein 1 subunit 5	A0AUT4	59	0	2	Protein folding
16	XlZPA protein	A1L3D9	78	0	2	Single fertilization
17	Peroxiredoxin-2	Q6ING3	22	0	1	cell redox homeostasis
18	Nucleoporin	Q6PAY1	55	0	1	transmembrane transport
19	Chaperonin containing TCP1, subunit 7	Q5XGK8	52	0	1	Protein folding
20	Calcineurin A	O57438	58	0	1	Cell division
21	Copin	Q6P7H2	59	0	1	vesicle-mediated transpor
22	Egg envelope glycoprotein	Q4VGP0	108	0	1	Unknown
23	Nupl1 protein	A4FU91	60	0	1	transmembrane transport
24	Hadh2-prov protein	Q6DCM8	27	0	1	oxidation reduction
25	Acad9-prov protein	Q6DDF2	68	0	1	oxidation reduction
26	Aldehyde dehydrogenase family 18, member A1	Q6GMF0	89	0	1	proline biosynthetic process
27	Egg envelope component ZPAX	B4F6R0	102	0	1	Unknown
28	LOC100049148 protein	A4QN33	95	0	1	Unknown
29	Thyroid hormone receptor-associated protein 3 (TRAP150)	Q5BJ39	108	0	1	regulation of transcription
30	MGC68559 protein	Q6PAA1	24	0	1	Calcium ion binding

Table 2: Potential interactors of CDK1 identified by mass spectrometry from CDK1 immunoprecipitation in activated *X. laevis* UFE (proteins highlighted in grey are common between metaphase II arrested and activated UFE)

	Protein name	Accession Number	Molecular Weight (kDa)	Unique peptide c- T7	Unique peptide IP T7	Biological process (GO annotation)
1	Kinectin 1	Q08B03	97	0	9	Microtubule-based movement
2	Cell division control protein 2-A	P35567	35	2	8	Cell division
3	Mitogen-activated protein kinase 1	P26696	41	0	4	Cell cycle
4	T-complex protein 1 gamma subunit	P50143	61	0	4	Protein folding
5	Heat Shock Protein A8	Q7ZTK6	71	1	4	ATP binding
6	Transitional endoplasmic reticulum ATPase	P23787	89	0	3	Transport
7	Histone deacetylase 10	Q569T0	77	0	3	hydrolase activity
8	Nucleoporin	Q6PAY1	55	0	3	transmembrane transport
9	Calcineurin A	O57438	58	0	3	Cell division
10	Copin	Q6P7H2	59	0	3	vesicle-mediated transport
11	Member of T-complex protein 1 chaperonin family	Q6GMA6	58	0	3	Protein folding
12	ATP synthase beta subunit	Q7ZWR6	56	0	3	ATP biosynthetic process
13	Hadh2-prov protein	Q6DCM8	27	0	3	oxidation reduction
14	Arginyl aminopeptidase	Q641C7	70	0	3	Proteolysis
15	Cyclin B2	Q6PA39	44	0	2	Cell division
16	Cell division control protein 2-B	P24033	35	0	2	Cell division
17	Chaperonin containing TCP1, subunit 7	Q5XGK8	52	0	2	Protein folding
18	RuvB like protein	Q0IH85	51	0	2	ATP binding
19	Nupl1 protein	A4FU91	60	0	2	transmembrane transport
20	Dynein, cytoplasmic 1, intermediate chain 2	Q5U238	72	0	2	Transport
21	Aldehyde dehydrogenase family 18, member A1	Q6GMF0	89	0	2	proline biosynthetic process
22	ATPase family AAA domain-containing protein 3-A	Q58E76	67	0	2	ATP binding
23	ATP synthase subunit alpha	Q68EY5	60	0	2	ATP biosynthetic process
24	Von Willebrand factor A domain containing 5A, gene 2	Q6IND5	94	0	2	Unknown
25	LOC733268 protein	Q0IH65	27	0	2	Unknown
26	Acyltransferase	Q642P5	54	0	2	fatty-acyl-CoA biosynthetic process
27	LOC431925 protein	Q6NR96	210	0	1	Proteolysis
28	Cyclin B4	Q98TI3	44	0	1	Cell division
29	Peroxiredoxin-2	Q6ING3	22	0	1	cell redox homeostasis
30	Sorcin	A2VDA2	22	0	1	Calcium ion binding
31	Heat shock protein d1	Q6IP60	62	0	1	Protein refolding
32	T-complex protein 1 subunit 5	A0AUT4	59	0	1	Protein folding
33	Acad9-prov protein	Q6DDF2	68	0	1	oxidation reduction
34	Nuclear pore glycoprotein	A2BDA4	50	0	1	transport
35	Ruvbl1 protein	Q6GR29	50	0	1	ATP binding

	Protein name	Accession Number	Molecular Weight (kDa)	Unique peptide c- T7	Unique peptide IP T7	Biological process (GO annotation)
36	Ratireb-prov protein	Q7ZY37	99	0	1	Metabolic process
37	Apx protein	B7ZSK3	159	0	1	Cell shape
38	Dlst-prov protein	Q7ZXF6	49	0	1	tricarboxylic acid cycle
39	Grp58-prov protein	Q7ZWU3	56	0	1	cell redox homeostasis
40	Pyruvate kinase	Q7ZY25	57	0	1	Glycolysis
41	Septin 9	Q498G4	39	0	1	Cell cycle
42	Nmp200-prov protein	Q7ZXW4	55	0	1	Protein ubiquitination

Table 3: Proteins identified by mass spectrometry from p9 precipitation in Metaphase II arrested *X. laevis* UFE (proteins highlighted in grey are common between metaphase II arrested and activated UFE)

	Protein name	Accession Number	Molecular Weight (kDa)	Unique peptide c- P9 T0	Unique peptide P9 T0	Biological process
1	Cell division control protein 2-A	P35567	35	0	9	Cell division
2	Heat shock protein A8	Q7ZTK6	71	0	6	ATP bindind
3	Cyclin B4	Q98TI3	44	0	5	Cell division
4	Cyclin B2	P13351	44	0	4	Cell division
5	Cyclin B5	Q5HZQ4	44	0	3	Cell division
6	Protein-L-isoaspartate O-methyltransferase	Q7SZS4	25	0	2	Protein modification process
7	Cell division control protein 2-B	P24033	35	0	2	Cell division
8	TRAF2 and NCK-interacting protein kinase	Q32NV8	57	0	2	Protein amino acid phosphorylation process
9	Cyclin B1	P13350	45	0	2	Cell division
10	Peroxiredoxin-2	Q6ING3	22	1	2	cell redox homeostasis
11	Galectin-VIIa	Q7ZSY1	28	0	1	sugar binding
12	XlGST Superfamily1-1 protein	Q7SZA7	23	0	1	Prostaglandin-D synthase activity
13	NIF3-like protein 1	Q0IHC9	37	0	1	Regulation of transcription
14	Ribosomal protein S30	Q4KLF0	15	0	1	Translation
15	Cofilin-1-A	P45695	19	0	1	Actin filament depolymerisation/ cytokinesis
16	CDK2	Q6IRQ7	34	0	1	Cell cycle
17	Double-stranded RNA-binding protein A	Q91836	33	0	1	RNA-mediated gene silencing
18	Heat shock protein a5	Q8AVE3	72	0	1	ATP bindind
19	Junction plakoglobin	P30998	82	0	1	Cell adhesion

Table 4: Proteins identified by mass spectrometry from p9 precipitation in activated *X. laevis* UFE (proteins highlighted in grey are common between metaphase II arrested and activated UFE)

	Protein name	Accession Number	Molecular Weight (kDa)	Unique peptide c- P9 T8	Unique peptide P9 T8	Biological process/molecular function
1	Heat shock protein A8	Q7ZTK6	71	1	9	ATP bindind
2	Cell division control protein 2-A	P35567	35	0	7	Cell division
3	Heat shock protein 9	Q7ZX34	73	0	4	ATP bindind
4	Protein-L-isoaspartate O-methyltransferase	Q7SZS4	25	0	3	Protein modification process
5	XlGSTS1-1	Q7SZA7	23	0	3	Prostaglandin-D synthase activity
6	Ferrochelatase, mitochondrial	O57478	46	0	3	heme biosynthetic process
7	Cyclin B2	P13351	44	0	2	Cell division
8	Cyclin B4	Q98TI3	44	0	2	Cell division
9	Peroxiredoxin-2	Q6ING3	22	0	2	cell redox homeostasis
10	Peptidyl-prolyl cis-trans isomerase	Q5XGR3	24	0	2	protein folding
11	NIF3-like protein 1	Q0IHC9	37	0	2	Regulation of transcription
12	Ribosomal protein S30	Q4KLF0	15	0	2	Translation
13	electron-transfer-flavoprotein, beta polypeptide	Q6PBB7	28	0	2	electron carrier activity
14	RNA terminal phosphate cyclase domain 1	Q6GMZ1	38	0	2	RNA processing
15	Galectin-VIIa	Q7ZSY1	28	0	1	sugar binding
16	Cofilin-1-A	P45695	19	0	1	Actin filament depolymerisation/ cytokinesis
17	Rpl3-prov protein	Q7ZYR1	46	0	1	Translation
18	CDK2	Q6IRQ7	34	0	1	Cell division
19	Cell division control protein 2-B	P24033	35	0	1	Cell division
20	TRAF2 and NCK-interacting protein kinase	Q32NV8	57	0	1	Protein amino acid phosphorylation process
21	Exportin-2	Q6GMY9	110	0	1	Protein transport
22	Double-stranded RNA-binding protein A	Q91836	33	0	1	RNA-mediated gene silencing
23	Hspa5 protein	Q8AVE3	72	0	1	ATP bindind
24	Uncharacterized protein KIAA0090	Q6NRB9	111	0	1	Unknown
25	Pyruvate kinase	Q6PA20	58	0	1	Glycolysis
26	Glucagon	B7ZQU9	25	0	1	Hormone activity
27	Small nuclear ribonucleoprotein Sm D3	P62323	14	0	1	mRNA processing

	Protein name	Accession Number	Molecular Weight (kDa)	Unique peptide c- P9 T8	Unique peptide P9 T8	Biological process/molecular function
28	Adenosylhomocysteinase B	O93477	48	0	1	one-carbon metabolic process
29	Egg envelope glycoprotein	Q4VGP0	108	0	1	Unknown
30	Embryonic polyadenylate-binding protein B	Q6GR16	71	0	1	mRNA processing
31	Nucleolin	B7ZR96	75	0	1	Nucleic acid binding
32	ATP synthase subunit alpha, mitochondrial	P08428	59	0	1	ATP biosynthetic process
33	O-6-methylguanine-DNA methyltransferase	Q8AVP6	35	0	1	DNA repair
34	ribosomal protein S27a	Q6GMC1	18	0	1	Translation
35	LOC414450 protein	Q6NTL7	13	0	1	Unknown
36	Caveolin	Q8AVS7	17	0	1	Various (e.g. vesicle trafficking, cholesterol homeostasis, signal transduction)
37	PKC-delta2 protein	Q498G7	78	0	1	signal transduction

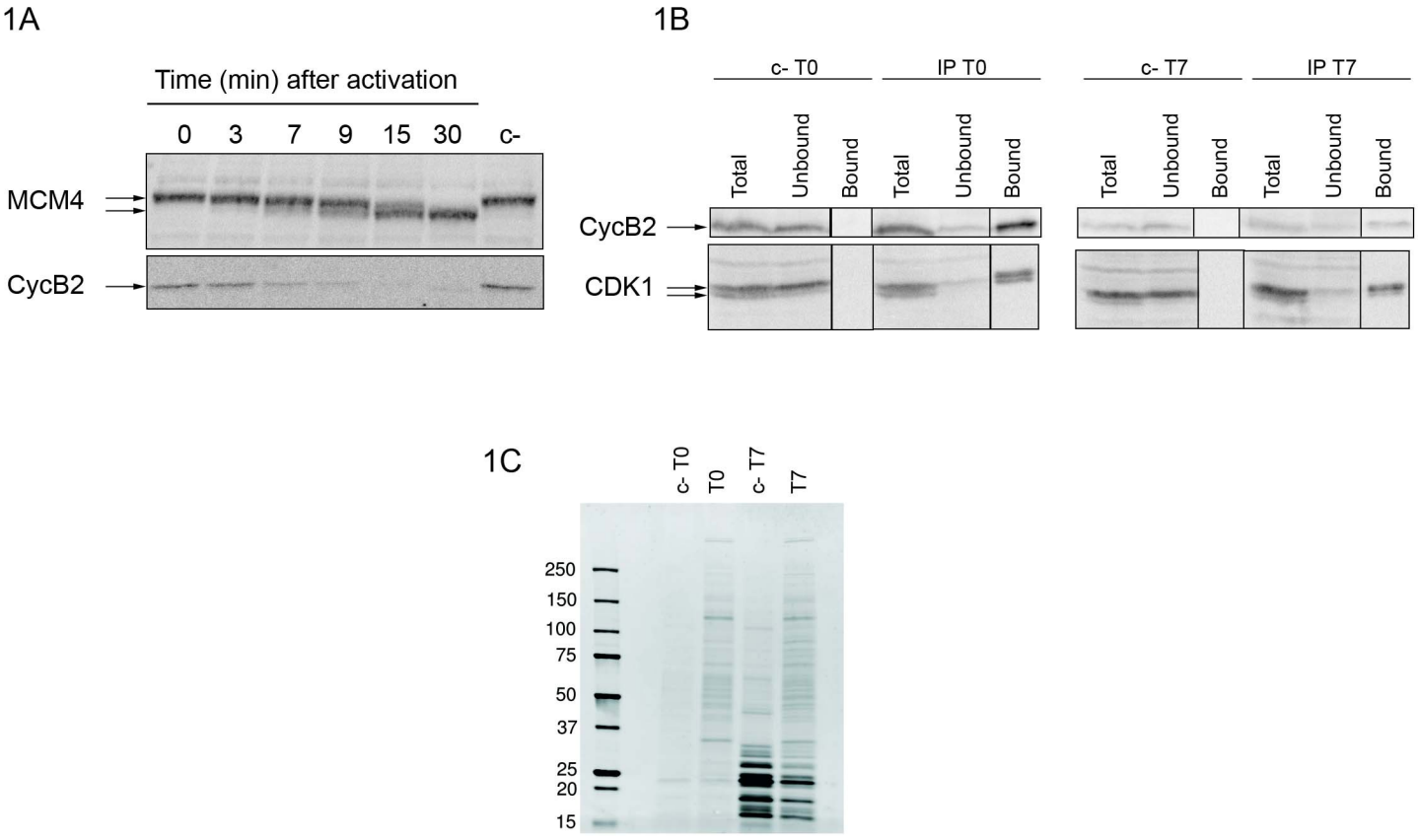
1A
Time (min) after activation
0 3 7 9 15 30 c-
MCM4
CycB2
1B
c- T0
IP T0
c- T7
IP T7
Total Unbound Bound Total Unbound Bound
Total Unbound Bound Total Unbound Bound
CycB2
CDK1
1C
c- T0
T0
c- T7
T7
250
150
100
75
50
37
25
20
15

Figure 1

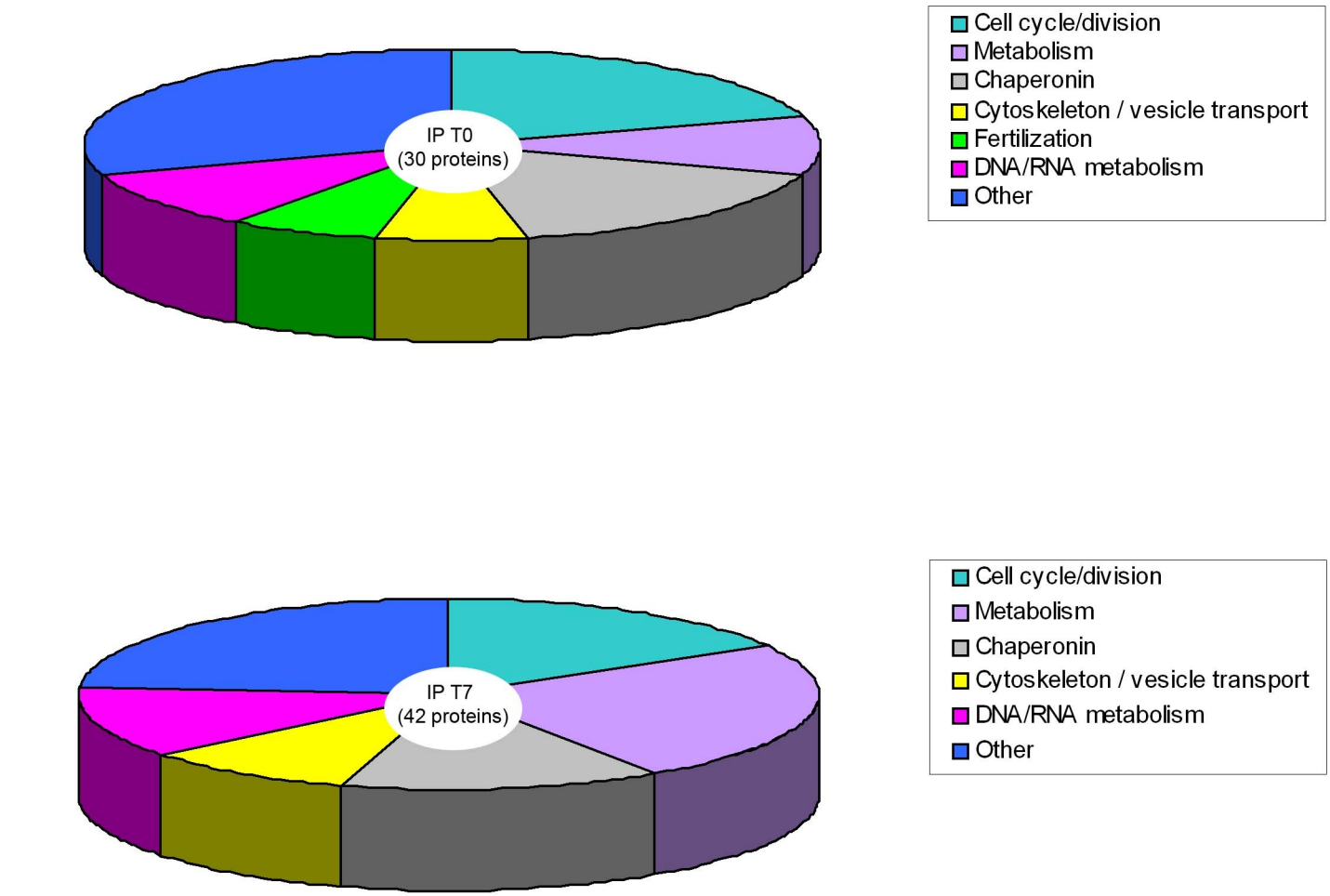
IP T0
(30 proteins)
Cell cycle/division
Metabolism
Chaperonin
Cytoskeleton / vesicle transport
Fertilization
DNA/RNA metabolism
Other
IP T7
(42 proteins)
Cell cycle/division
Metabolism
Chaperonin
Cytoskeleton / vesicle transport
DNA/RNA metabolism
Other

Figure 2

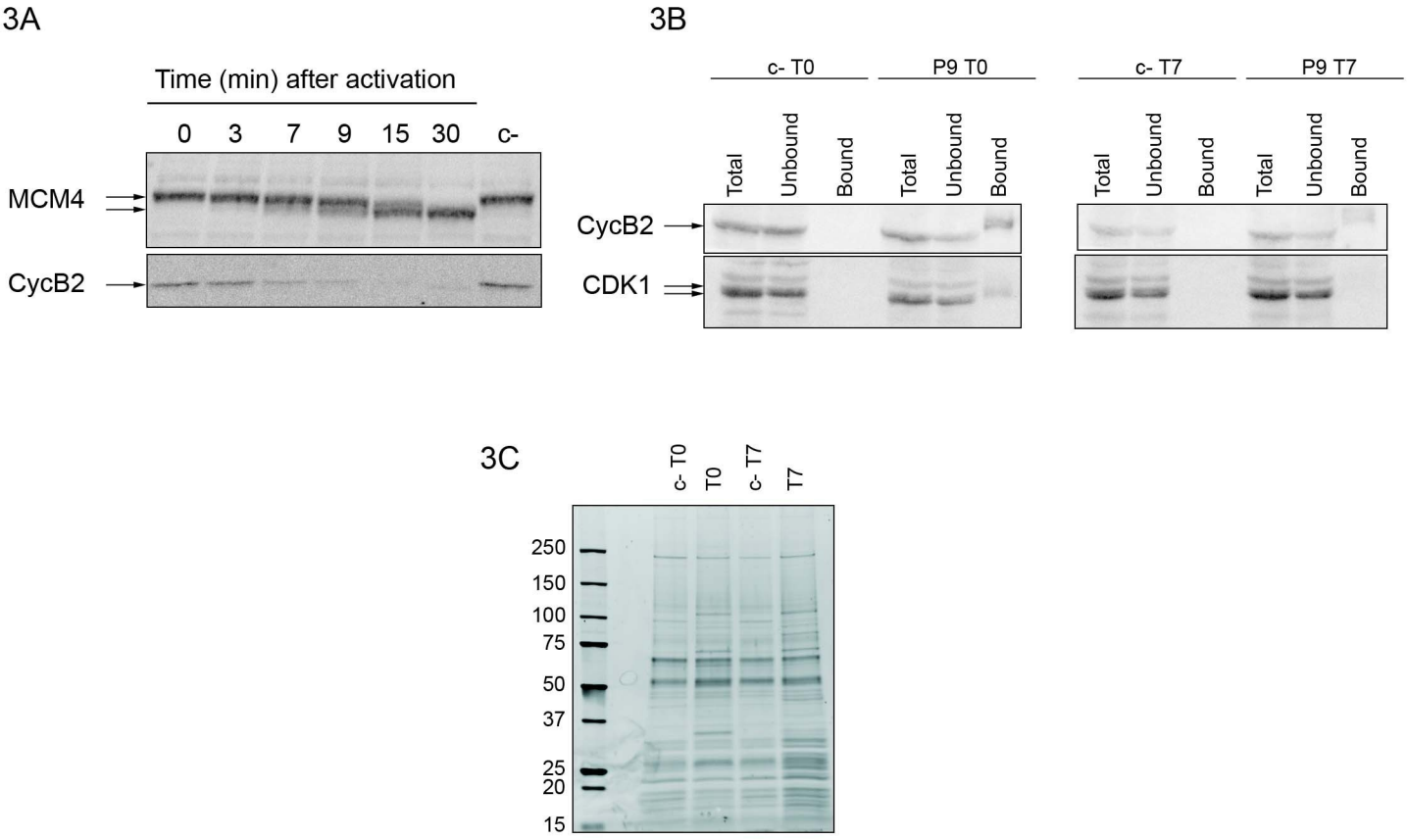
3A
Time (min) after activation
0 3 7 9 15 30 c-
MCM4
CycB2
3B
c- T0
P9 T0
c- T7
P9 T7
Total Unbound Bound Total Unbound Bound
Total Unbound Bound Total Unbound Bound
CycB2
CDK1
3C
c- T0
T0
c- T7
T7
250
150
100
75
50
37
25
20
15

Figure 3

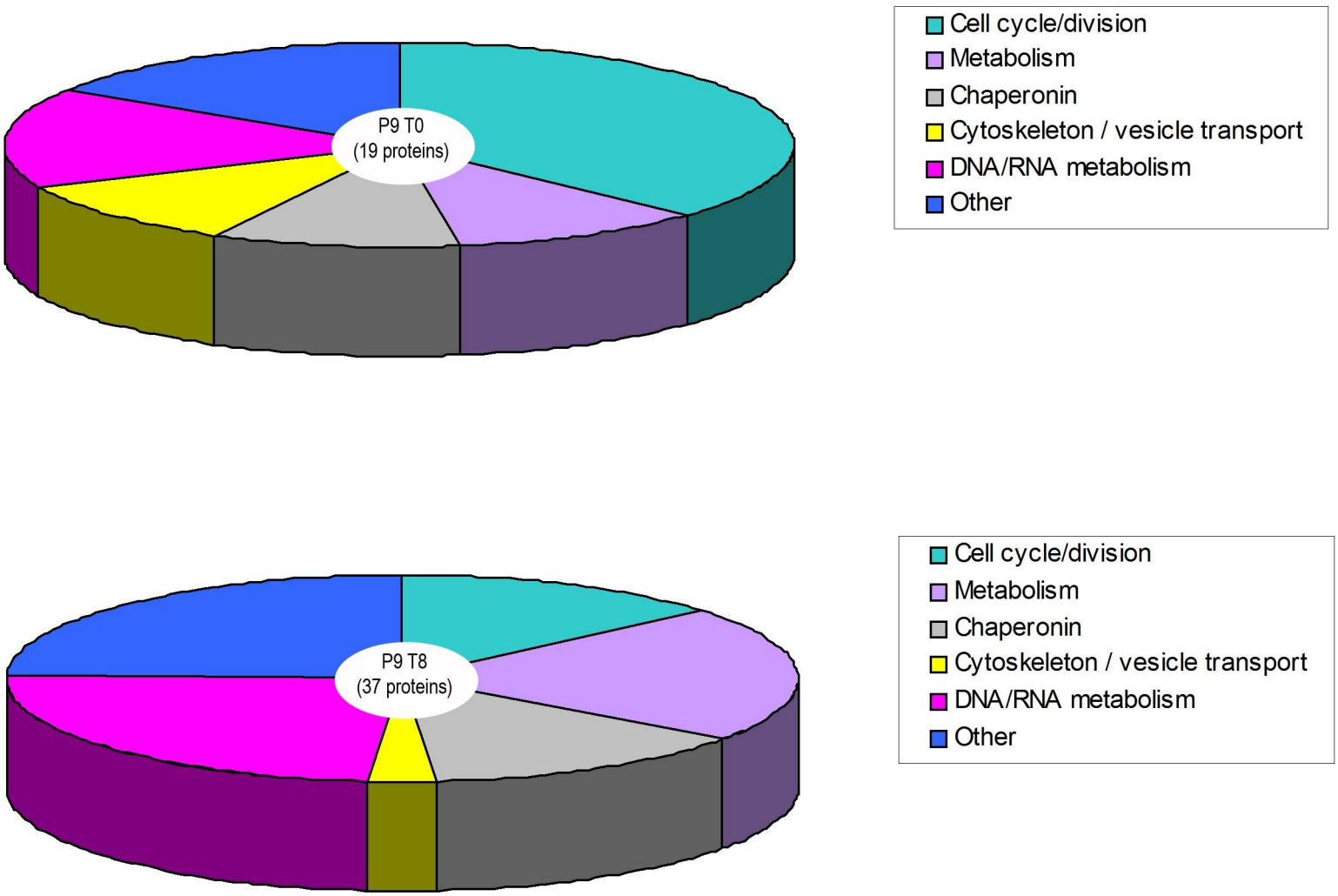
P9 T0
(19 proteins)
Cell cycle/division
Metabolism
Chaperonin
Cytoskeleton / vesicle transport
DNA/RNA metabolism
Other
P9 T8
(37 proteins)
Cell cycle/division
Metabolism
Chaperonin
Cytoskeleton / vesicle transport
DNA/RNA metabolism
Other

Figure 4

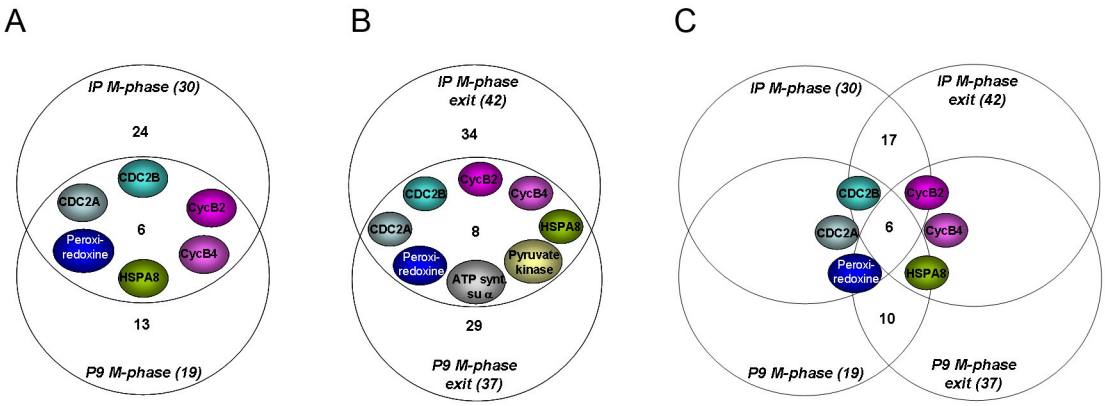
A
IP M-phase (30)
24
CDC2B
CDC2A
CycB2
Peroxi-redoxine
6
CycB4
HSPA8
13
P9 M-phase (19)
B
IP M-phase exit (42)
34
CycB2
CDC2B
CycB4
HSPA8
CDC2A
8
Peroxi-redoxine
Pyruvate kinase
ATP synt su α
29
P9 M-phase exit (37)
C
IP M-phase (30)
IP M-phase exit (42)
17
CDC2B
CycB2
CDC2A
6
CycB4
Peroxi-redoxine
HSPA8
10
P9 M-phase (19)
P9 M-phase exit (37)

Figure 5